

# Influence of in Vitro Degradation of a Biodegradable Nanocomposite on Its Shape Memory Effect

Xiongjun Yu, Shaobing Zhou,\* Xiaotong Zheng, Yu Xiao, and Tao Guo

School of Materials Science and Engineering, Key Laboratory of Advanced Technologies of Material, Minister of Education, Southwest Jiaotong University, Chengdu, 610031, Sichuan, P. R. China

Received: March 15, 2009; Revised Manuscript Received: August 27, 2009

Preparation and in vitro degradation of shape memory nanocomposites consisting of cross-linked poly( $\epsilon$ -caprolactone) (c-PCL) and  $\text{Fe}_3\text{O}_4$  nanoparticles were investigated in this study. The degradation behaviors were evaluated from the decrease of mechanical property, weight, and molecular weight of polymer, the change of pH value of phosphate-buffered saline (PBS), and morphological changes in composites. The results from gel fraction and molecular weight analysis indicated some damages were brought to chemical networks of c-PCL, but its linear molecule configuration received less impact from PBS degradation medium. Expectedly, the negative influence of the in vitro degradation on shape memory effect had been observed. All these physical and chemical properties related to degradation had been tested to analyze degradation behaviors, which were further used to explain the changes in shape memory recovery. Furthermore, on the basis of the degradation results, the mechanism of c-PCL degradation was also put forward to illustrate the effect of degradation on shape memory. This research will supply a guideline for effectively using and preserving biodegradable shape memory composites.

## Introduction

Biodegradable shape memory polymers (SMPs) for biomedical application have already obtained rapid development in recent years just because of their excellent comprehensive performance or multifunctionality (e.g., shape memory capability and biodegradability).<sup>1</sup> This type of multifunctionality is especially advantageous when used for minimally invasive surgery<sup>2</sup> and as intelligent suture for wound closure.<sup>3</sup> Biodegradation of SMPs can be realized by cleaving weak, hydrolyzable bonds in macromolecules under physiological conditions, and thus be beneficial to avoid secondary surgery if the polymers were used for medical instruments. Henceforth, biodegradable SMPs aroused noticeable interest in study and application. Common biodegradable polymers that can be used to prepare SMPs refer to the polyester family (e.g., polycaprolactone,<sup>4</sup> polylactide,<sup>5</sup> poly(dioxanone))<sup>3,6</sup> and the copolymers<sup>7,8</sup> related to them.

Until now, many researchers have studied the shape memory effect (SME) from these biodegradable polymers. Heat-induced SMPs, as a branch of the SMP family, can show their shape recovery using direct heat stimulation, and also the shape memory effect may be tuned via tailoring materials' molecular weight,<sup>9</sup> proportion of component,<sup>10,11</sup> temperature,<sup>12,13</sup> dimension,<sup>14</sup> loading recycle times,<sup>15</sup> recovery time,<sup>16</sup> and so forth. For novel SMPs, application of light,<sup>17</sup> electrical voltage,<sup>18</sup> and electromagnetic field<sup>19</sup> has been studied to stimulate SME. All the research demonstrated a variety of approaches to improve SME. In spite of this, the research only focused on shape memory effect of SMPs before they were used in medicine. Inevitably, some biological or physical properties, especially SME, would change when these materials were used as implant devices considering their degradability. If the SME decreases

and even disappears during their degradation, their application must be influenced or even limited in the biomedical field. However, to our knowledge, by this time there is some literature investigating the change in SME of these SMPs with polymer degradation. Herein, the influence of in vitro degradation on its SME was studied, which could supply some important data for better preserving and using SMPs.  $\text{Fe}_3\text{O}_4$  nanoparticles (NPs) were typically employed as a biomedical material because of their favorable biocompatibility and availability.<sup>20</sup>  $\text{Fe}_3\text{O}_4$  NPs were used to introduce magnetic sensitivity into SMPs made from cross-linked PCL (c-PCL) to obtain the magnetic field-induced shape memory effect in our previous report.<sup>21</sup> As a further study, the current work investigated the influence of in vitro degradation on SME of c-PCL and c-PCL/ $\text{Fe}_3\text{O}_4$  nanocomposites with 5 and 15 wt %  $\text{Fe}_3\text{O}_4$ .

Three classes of specimens (c-PCL, c-PCL/ $\text{Fe}_3\text{O}_4$  with 5 and 15 wt %  $\text{Fe}_3\text{O}_4$ ) were prepared to investigate the effect of  $\text{Fe}_3\text{O}_4$  filler on in vitro degradation and the effect of the degradation on shape memory behavior of these nanocomposites. Some important properties (e.g., mechanical property, molecular weight, and gel fraction) were tested to trace degradation behavior of specimens. The mechanism of shape memory behavior was also illustrated on the basis of the degradation.

## Experimental Section

**Materials.** Linear PCL was synthesized in our lab as previous reported.<sup>22</sup> The molecular weight measured by Waters2695/2414 gel permeation chromatography (GPC, Waters) was 112 000 Da. The biocompatible  $\text{Fe}_3\text{O}_4$  magnetite nanoparticles were synthesized according to a chemical coprecipitation method.<sup>23</sup>

**Preparation of Shape Memory Polymer and Its Nanocomposites.** The preparation of c-PCL was as follows. First, preweighed pristine PCL and benzoyl peroxide (BPO) as initiator were dissolved in chloroform separately. Then, BPO solution was injected into PCL under stirring, and to procure

\*To whom correspondence should be addressed. Telephone: 86-28-87634023. Fax: 86-28-87634649. E-mail: shaobingzhou@swjtu.edu.cn; shaobingzhou@hotmail.com.

pristine PCL/BPO composites, the PCL/BPO mixture solutions were kept in aerator overnight and further dried under vacuum condition for 10 h. Finally, the dried PCL/BPO composites were subjected to press-molding at 120 °C for 10 min in a mold. Therefore, c-PCL sheets with about 0.2-mm thickness could be obtained because BPO enables cross-linking reaction to occur at 120 °C.

The preparation of both composite strips can be described as follows. First, 10% (wt %) pristine PCL/BPO solution in chloroform and an uniformly dispersed system of 1% (wt %)  $\text{Fe}_3\text{O}_4$ /xylene were prepared. Second, both were mixed by stirring and ultrasonic dispersion to reduce  $\text{Fe}_3\text{O}_4$  NPs congregating, and some conglomerations were separated out from solvent by adding ethanol. Finally, after the conglomerations were dried, composite sheets (c-PCL/ $\text{Fe}_3\text{O}_4$ ) could be prepared through press-molding as described above.

**In Vitro Degradation.** First, rectangle-shaped strips with dimension of 50 mm  $\times$  5 mm  $\times$  0.2 mm (length  $\times$  width  $\times$  thickness) and dumbbell-shaped strips with dimension of 60 mm  $\times$  40 mm  $\times$  10 mm  $\times$  4 mm (length overall  $\times$  length of narrow section  $\times$  width overall  $\times$  width of narrow section) were cut from c-PCL sheets. Next, the two groups of samples were immersed in PBS and kept at  $37 \pm 1$  °C. Finally, a specimen in each group was taken out at an interval of two weeks and dried, followed by various tests (i.e., shape memory effect, microstructure morphology, mechanical property, pH value, weight loss, gel percentage, and molecular weight analysis).

The degradation experiments of c-PCL/ $\text{Fe}_3\text{O}_4$  with 5 and 15 wt %  $\text{Fe}_3\text{O}_4$  were almost similar to the above method. However, it should be pointed out that a centrifugal program must be added to collect the specimens since some observable floccules from the specimen strip during degradation.

**Characterization.** In this study, shape recovery was stimulated by hot water at 55 °C. First, an initial length,  $L_0$ , was noted before measure of shape recovery. Second, the specimens were heated for 1 min so that they were softened, followed by a slow stretch applied to the specimens with a couple of clamps to get a temporary shape with the length of  $L_1$ . Third, the temporary shape was frozen in an ice–water mixture of 0 °C for 1 min. Fourth, shape recovery of the specimens could promptly happen, and the steady length of  $L_2$  could be achieved when the frozen specimen was reheated in the hot water. Finally, recovery ratio,  $R_r$ , could be determined as follows:

$$R_r = (L_1 - L_2)/(L_1 - L_0) \times 100\% \quad (1)$$

The combination degree between  $\text{Fe}_3\text{O}_4$  NPs and their c-PCL matrix can be observed by scanning electron microscope (SEM, FEI), and simultaneously the dispersibility of NPs embedded in polymer matrix can be supplied.

A static tensile test was accomplished using a universal testing machine Instron 5567 (Instron Company) at the crosshead speed of 5 mm/min at room temperature. Of all the mechanical properties, Young's modulus  $E$  and tensile strength  $\sigma_b$  were investigated.

The pH value of PBS degradation medium was measured using a pH meter, and weight loss of polymer matrix was estimated by comparing the weight before and after the degradation.

A molecular weight test was carried out to monitor the degradation process. Briefly, specimens were immersed in tetrahydrofuran to separate the gel and sol, and then the sol was further decontaminated by centrifuge for GPC test.

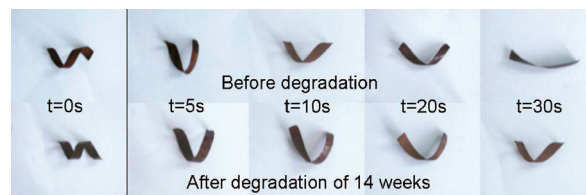


**Figure 1.** Photographs showing the process of shape memory recovery of c-PCL/ $\text{Fe}_3\text{O}_4$  ( $\text{Fe}_3\text{O}_4$  content: 15%) before and after in vitro degradation.

A cross-linking degree can be estimated as follows. In brief, the specimen with preweighed  $M_0$  was immersed in chloroform in a centrifuging tube for 24 h, and then an injector was used to extract the solution from the sol–gel mixture system. The gel was washed three times with chloroform and dried in the vacuum overnight to remove solvent. A residual weight of dried gel was noted,  $M_g$ , and gel percentage could be calculated by the following formula:

$$\text{Gel\%} = M_g/M_0 \times 100\% \quad (2)$$

## Results and Discussion

**Shape Memory Property.** Figure 1 gives a visual comparison of shape recovery effect before and after c-PCL/ $\text{Fe}_3\text{O}_4$  experienced in vitro degradation of 14 weeks. Photos of two helix strips were taken with a digital camera to show the shape recovery progress. An excellent shape recovery could be observed on the specimens before degradation. However, an obvious decline on it was also observed after the composites were incubated in PBS for 14 weeks, as shown in Figure 1, which indicated that there may be some damages to interfacial combination and chemical networks of the nanocomposites because of polymer matrix degradation.

It is well-known that, in principle, SME comes from two phases in the polymer or composites. The phases are composed of reversible phase, typically characterizing glass transition and melting behavior, and fixable phase characterizing crystallites and chemically cross-linking points that function as a role of memorizing initial shape. On heating, the reversible phase is actuated and then starts to transition to other phases when ambient temperature is close to the glass transition temperature ( $T_g$ ) or melting temperature ( $T_m$ ) of polymer. In macroscopic view, specimens start softening and come to a rubbery state so that they can be deformed to a desired temporary shape owing to reversible phase transition. Then, the temporary shape was promptly frozen at a temperature lower than that at which the reversible phase was actuated. During deformation, the outside force was stored in the whole region of specimens and then frozen together with shape. When reheating was employed, the frozen stress will be released again to pull the activated but ordered polymeric macromolecule chains to a more random state, and thus, a macroscopic shape recovery is represented on the shape memory polymers or polymer-based composites. This shape recovery is related to entropy elasticity of polymer.<sup>24</sup> Typically, for a complex system composed of NPs filler and polymer matrix, there exist several possible factors that can potentially affect stress storage and in turn shape recovery. Of all the factors that can affect stress storage, interfaces of fillers/matrix and chemical network would play important roles in determining shape recovery. The explanation for this could be described as the contribution of chemical and physical network to stress storing by decreasing stress relaxation in virtue of more

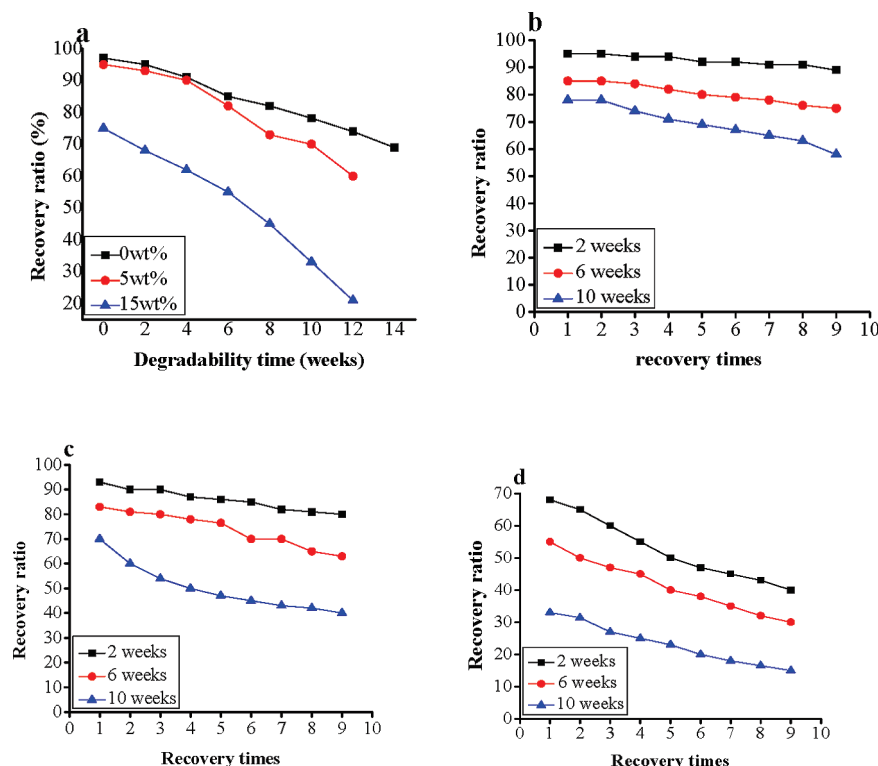


**Figure 2.** Shape recovery effect versus degradation time (a) and loading recycle times (b, c, and d) for the nanocomposites with 0, 5, and 15 wt %  $\text{Fe}_3\text{O}_4$  nanoparticles, respectively ( $n = 3$ ).

“bridge” among polymeric molecules or between molecule and filler in composites. While investigating shape recovery, we found that the “bridge” can work as fixable phase to memory initial shape. In our complex system consisting of  $\text{Fe}_3\text{O}_4$  NPs and c-PCL, the reversible phase concretely refers to PCL crystallites, and the fixable phase refers to network structures (i.e., chemical network structure in PCL matrix and physical network of NPs-PCL as the polyurethane–glass fiber composites have).<sup>25</sup> Therefore, the shape recovery of c-PCL and c-PCL/ $\text{Fe}_3\text{O}_4$  may be affected by the interface between  $\text{Fe}_3\text{O}_4$  NPs and PCL as physical fixable phase, and PCL network structures as chemical fixable phase since the phases would change during its degradation. In fact, the contribution of chemical network to shape recovery has been confirmed in our previous report where the relationship between gel fraction and shape recovery of polymer before degradation has been discussed in detail.<sup>21</sup>

On the basis of the above analysis, the influence of degradation on shape recovery was studied as a key part of this study. In this part, we explored the influence of the degradation time and load times on shape recovery of the nanocomposites. Figure 2a shows that all the specimens with  $\text{Fe}_3\text{O}_4$  of 0, 5, and 15 wt % represented a similar decreasing tendency in shape recovery. For the specimen without  $\text{Fe}_3\text{O}_4$ , namely c-PCL, it had the slowest decrease in shape recovery among the three samples, and when 5 wt %  $\text{Fe}_3\text{O}_4$  was incorporated, the decline of shape recovery was more obvious after six weeks' degradation although it was familiar with c-PCL in the first six weeks. Distinctly, the specimen with 15 wt %  $\text{Fe}_3\text{O}_4$  had a disillusionary decline in SME during degradation. For example, the recovery had decreased from 75% before degradation to 20% at the twelfth week. An important illustration on the profile must be noted that the recovery rates of both composites after 14 weeks' degradation had not been supplied just because the composites strips were prone to break during shape recovery measure, and so, the study on degradation for a longer time did not go on.

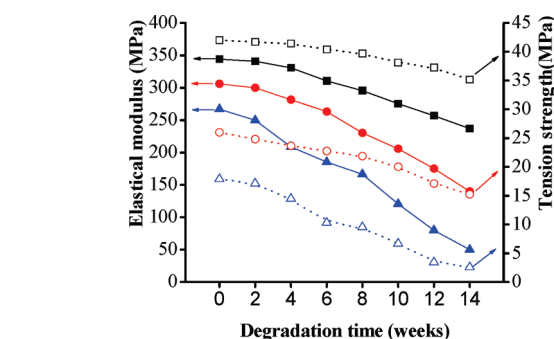


**Figure 3.** Tension strength  $\sigma_b$  and elastic modulus  $E$  function versus degradation time. (■, □) Samples with 0 wt %  $\text{Fe}_3\text{O}_4$  nanoparticles. (●, ○) Samples with 5 wt %  $\text{Fe}_3\text{O}_4$  nanoparticles. (▲, △) Samples with 15 wt %  $\text{Fe}_3\text{O}_4$  nanoparticles ( $n = 3$ ).

Recovery functions of the specimens versus load times are also exhibited in Figure 2b–d. From the figure, it could be found that the specimen with 15 wt %  $\text{Fe}_3\text{O}_4$  had the fastest decline in shape recovery but the decline was slowest for the c-PCL during the degradation. This may be ascribed to the fact that residual networks in the specimens would tend to be further damaged, resulting in producing more breakpoints in PCL macromolecule chains when the specimens were reheated and loaded repeatedly. This result indicated that degradation time had the most effect on shape recovery. One reason was that the physical interaction between  $\text{Fe}_3\text{O}_4$  NPs and PCL had been weakened so that the physical network had been damaged because the degradation medium penetrated into the composites, and the other was that the chemical network was damaged as proved in the gel percentage analysis which could affect shape recovery as a chief aspect. The two damaged networks had brought a decrease in shape recovery.

**Mechanical Property.** For the composite composed of inorganic filler and polymeric matrix, it could be assumed by



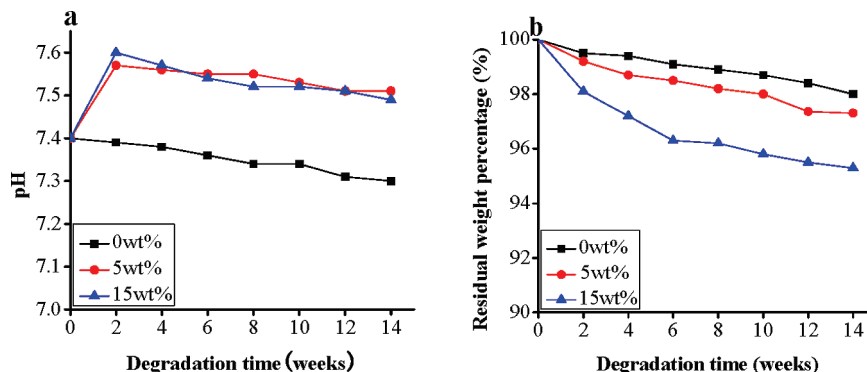


Figure 4. Residual weight percentage (a) and pH value (b) versus degradation time, respectively ( $n = 3$ ).

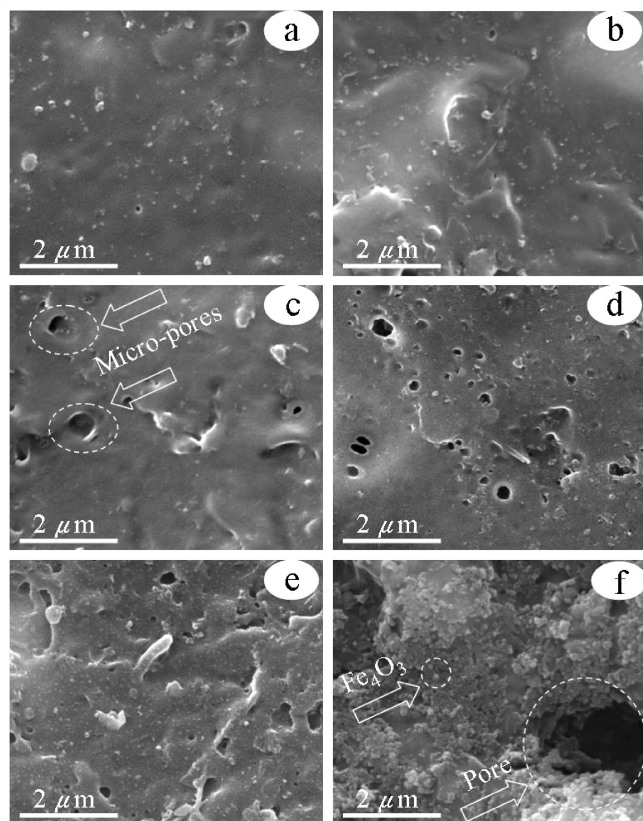


Figure 5. Morphological changes during the degradation processing obtained from SEM photos a, b, c, d, e and f taken when the 15 wt % composites experienced degradation for 0, 2, 6, 10, and 14 weeks, respectively.

common sense that phase interfaces would play a crucial role in determining mechanical property. In this view, a static mechanical property test was performed, which proved the influence of the *in vitro* degradation since interface property between PCL and  $\text{Fe}_3\text{O}_4$  NPs could bring a potential effect on mechanical properties. It is shown in Figure 3 that all the specimens behaved the same downtrend with the degradation time, and, moreover, with  $\text{Fe}_3\text{O}_4$  NPs increasing in composites, the downtrend was more and more remarkable. The result also indicated that the  $\text{Fe}_3\text{O}_4$  NPs played an important role in the downtrend of  $E$  and  $\sigma_b$ . In recent years, some factors had been considered to analyze the properties of composites (e.g., molecular mass of polymeric matrix<sup>26</sup> and concentration,<sup>25</sup> species shape,<sup>27</sup> size of fillers,<sup>28</sup> and mixing method).<sup>29</sup> In our system, molecular mass of PCL matrix and concentration of  $\text{Fe}_3\text{O}_4$  has also been used to explain the above results. The change in chemical network and physical network in c-PCL/

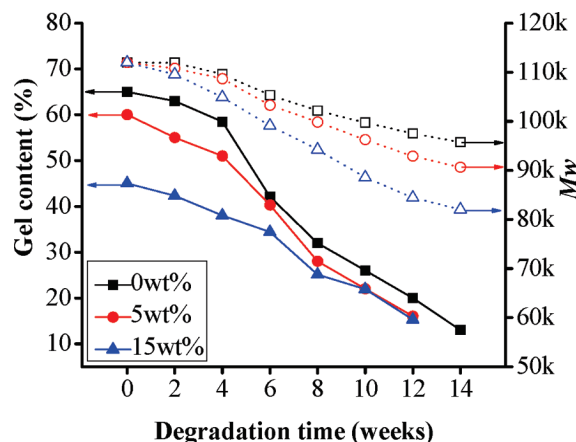
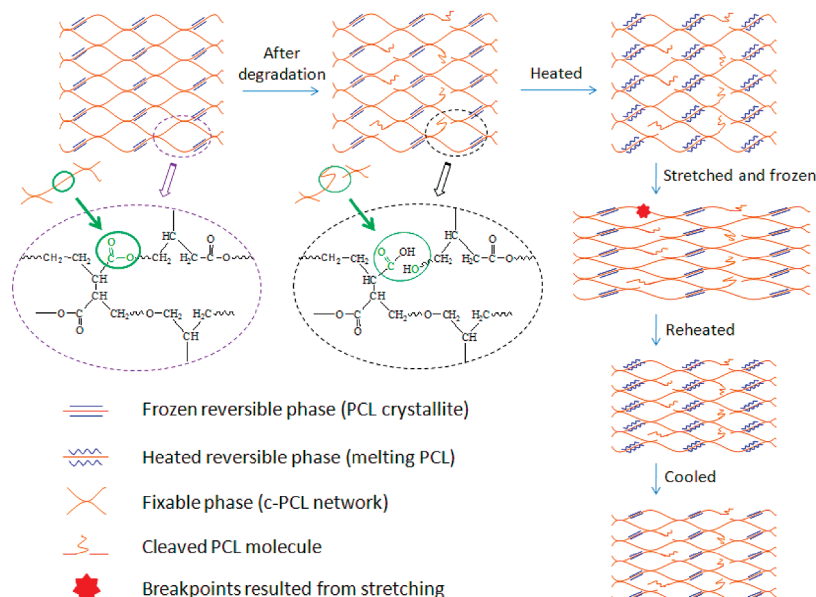


Figure 6. Average molecule weight and gel percentage function versus degradation time. As with the mechanical property, the dates of both composites with 5 and 15 wt %  $\text{Fe}_3\text{O}_4$  nanoparticles have not been supplied because little gel can be extracted when they experienced degradation for 14 weeks ( $n = 3$ ).

$\text{Fe}_3\text{O}_4$  could lead to a deconstructive effect on the mechanical property. Additionally,  $\text{Fe}_3\text{O}_4$  could facilitate pervasion of degradation medium into PCL networks, and thus a more serious damage to the interface was brought and even some obvious floccules could be observed in the medium. This can be explained by the theory of invasive effect and surface energy that was given by Zisman.<sup>30</sup> However, a much smaller influence of the degradation on the mechanical properties of composite could be observed for the residual linear PCL, which was mainly due to its slow degradation.

#### pH Value Decrease and Weigh Loss with Degradation.

To further confirm the above results, the conventional evaluations (e.g., the change in pH value of PBS and weight of composites) were also used to investigate the degradation. In theory, if the ester linkages in PCL were randomly cleaved by hydrolysis, pH values of aqueous medium will decrease owing to the presence of the acidic degradation products. In the view, the pH value in the current study would have a continuous decrease from the beginning of 7.40. On the contrary, some unexpected results had been obtained, as shown in Figure 4. The pH values for both composites showed an unexpected increase after degradation for two weeks and then a slow decreasing tendency, but pH value for c-PCL had been declining since the degradation started, as shown in Figure 4a. The weight loss profile (Figure 4b) showed a slower decreasing pace owing to PCL semicrystallinity<sup>31</sup> and hydrophobicity. However, for the composites with 5 and 15 wt %  $\text{Fe}_3\text{O}_4$  NPs, the changes in these values were more evident when compared with the pure c-PCL. Furthermore, the degradation rate increased with the



**Figure 7.** Scheme of shape recovery progress. The diagram demonstrates that the cleaved PCL molecule would bring a negative effect on shape memory effect for the specimens that experienced in vitro degradation.

content of  $\text{Fe}_3\text{O}_4$  increase. The result also agreed with the above results. A complex system consisted of hydrophilic  $\text{Fe}_3\text{O}_4$ , and hydrophobic polymeric matrix has a more probable tendency to absorb aqueous medium than pure polymer. This implied that  $\text{Fe}_3\text{O}_4$  could facilitate the infiltration of degradation medium into composite and thus promote its degradation. On the other hand, because of slow degradation of c-PCL, alkaline  $\text{Fe}_3\text{O}_4$  may neutralize the acidic environment from the degradation product of PCL, and in turn increase the pH value of PBS medium just like our prior study on PDLL/ $\beta$ -tricalcium composites.<sup>32</sup>

**Microstructure Morphology.** To further analyze the influence of the degradation on SME, the microstructure change of the composites was investigated. As a class of typical specimen, the nanocomposite with 15 wt %  $\text{Fe}_3\text{O}_4$  was subjected to accomplish analysis of surface morphology to trace the degradation behavior. Figure 5 gives a series of SEM photos of the composite to illustrate the gradual degradation involvement. Comparing panels a and b of Figure 5, the specimen strip still had a smooth surface after the first two weeks, which illustrates a slow degradation for the strip. However, Figure 5c–e shows that increasing drawback (e.g., flaw and micropores) had emerged in the strip because of the degradation of polymer matrix, and some observable pores had come into being after six weeks' degradation. Especially, after degradation for 14 weeks, many observable pores had been formed and many nanoparticles had been exposed in the strip (Figure 5f), which might bring an undesired effect on other properties including mechanical property and shape recovery property. The generation of pores would also cause a decrease of interfacial interaction between polymer matrix and nanoparticles, and thus might accelerate degradation of composites' interior. This demonstrates that PCL is of a homogeneous degradation that simultaneously occurs outside and inside of composite strips. However, the physical interaction between  $\text{Fe}_3\text{O}_4$  and PCL had been weakened, which must bring a negative effect on shape recovery since the physical fixable phases were weakened. Another fact that may be observed about the  $\text{Fe}_3\text{O}_4$  NPs is that they had quasi-sphericity in shape and integrated with surrounding PCL matrix tightly, which may contribute to SME before degradation.

**Gel Percentage and Molecular Weight.** In this study, PCL macromolecule as polymer matrix has two aggregate structures: physically tangling and chemically covalently cross-linking network. Considering their effects on shape recovery behavior of composites, their corresponding molecular weight and gel percentage were measured during degradation. As shown in Figure 6, molecular weight and gel percentage relationships with degradation time were given, respectively. Molecular weight provided by GPC test showed a slow decreasing tendency versus degradation time whereas the presence of hydrophilic  $\text{Fe}_3\text{O}_4$  can facilitate PBS medium infiltration and in turn accelerate the PCL degradation. It is well-known that PCL is of full breakdown time of up to 2 years under physiological conditions,<sup>33</sup> which could support our result. However, gel percentage showed a more obvious descending trend since the cleaved ester bonds had led the cross-linking degree to decreasing. Taking c-PCL, for instance, the gel percentage experienced a decline from 65% before degradation to 42.1% after six weeks. Compared to the change in molecular weight, gel percentage analysis further implied that chemical network had a more obvious effect on SME,<sup>4</sup> and therefore, in this study, the decreasing shape recovery was mainly attributed to impaired chemical network.

**Scheme of Shape Memory Progress.** To further illustrate the results in the microcosmic level, a scheme was supplied as shown in Figure 7. From the figure, the damaged chemical network resulting from polymer chain cleavage was used to explain the change in shape memory effect. The fixable phase, a perfect chemical network, had come into being by using press-molding at 120 °C in the presence of a cross-linking agent, and plenty of ester bonds were kept in cross-linking chains. However, the ester bonds would also be gradually cleaved when they experienced in vitro degradation in PBS medium, which had caused serious damage to the fixable phase resulting in shape recovery decreasing. This corresponded to the breakpoints in PCL molecule chains in the schematic diagram. By the diagram, we could illustrate the nature of the influence of degradation of c-PCL on its shape memory effect.

## Conclusions

In summary, the influence of the in vitro degradation of polymer on its shape memory effect was investigated. The

change in shape recovery with degradation time had revealed a decreasing tendency for the three types of specimens, and the effect in load times on shape recovery was similar to that of degradation time. Additionally, all composites had a faster decline in shape memory effect than pure c-PCL because of the presence of  $\text{Fe}_3\text{O}_4$ , and in particular, the composite with 15 wt %  $\text{Fe}_3\text{O}_4$  was the most obvious. The degradation results indicated that the degradation rate increased with the addition of  $\text{Fe}_3\text{O}_4$  in composites because of the nanoparticle hydrophilicity. The nature of c-PCL degradation is still that degradation is triggered by water that hydrolyzes the functional groups (ester bonds).<sup>34</sup> The results from microstructure and gel fraction analysis indicated that, for c-PCL, the ester bonds located cross-linked chains that were simultaneously degraded, which caused some damages to fixable phase and further led the shape memory effect to decrease. On the basis of the results, a scheme was designed to illustrate the degradation mechanism and the effect of the degradation on shape memory of c-PCL. It is necessary to perform the study and widen the study to other biodegradable polymers because the results can give us a guide to select SMP as implant devices.

**Acknowledgment.** This work was partially supported by the National Natural Science Foundation of China (50773065), Programs for New Century Excellent Talents in University, Ministry of Education of China (NCET-07-0719), and Sichuan Prominent Young Talent Program (08ZQ026-040).

## References and Notes

- (1) Feninat, F. E.; Laroche, G.; Fiset, M.; Mantovani, D. *Adv. Eng. Mater.* **2002**, *4*, 91–104.
- (2) Lendlein, A.; Kelch, S. *Mater. Sci. Forum* **2005**, *492–493*, 219–224.
- (3) Lendlein, A.; Langer, R. *Science* **2002**, *296*, 1673–1676.
- (4) Zhu, G.; Liang, G.; Xu, Q.; Yu, Q. *J. Appl. Polym. Sci.* **2003**, *90*, 1589–1595.
- (5) Zini, E.; Scandola, M. *Biomacromolecules* **2007**, *8*, 3661–3667.
- (6) Rickert, D. *Clin. Hemorheol. Microcirc.* **2005**, *32*, 117–128.
- (7) Meng, Q.; Hu, J.; Zhu, Y.; Lu, Y.; Liu, Y. *J. Appl. Polym. Sci.* **2007**, *106*, 2515–2523.
- (8) Meng, Q.; Hu, J. *Polym. Adv. Technol.* **2008**, *19*, 131–136.
- (9) Chen, S.; Hu, J.; Liu, Y.; Liem, H.; Zhu, Y.; Meng, Q. *Polym. Int.* **2007**, *56*, 1128–1134.
- (10) Zhu, Y.; Hu, J.; Yeung, L. Y.; Lu, J.; Meng, Q.; Chen, S.; Yeung, K. W. *Smart Mater. Struct.* **2007**, *16*, 969–981.
- (11) Meng, Q.; Hu, J.; Zhu, Y. *J. Appl. Polym. Sci.* **2007**, *106*, 837–848.
- (12) Khonakdar, H. A.; Jafari, S. H.; Rasouli, S.; Morshedani, J.; Abedini, H. *Macromol. Theory Simul.* **2007**, *16*, 43–52.
- (13) Miaudet, P.; Derré, A.; Maugey, M.; Zakri, C. *Science* **2007**, *318*, 1294–1296.
- (14) Zheng, X.; Zhou, S.; Li, X.; Weng, J. *Biomaterials* **2006**, *27*, 4288–4295.
- (15) Li, J.; James, A. V.; Michelle, H. W.; Anthamatten, M. *Adv. Mater.* **2007**, *19*, 2851–2855.
- (16) Liu, Y.; Chung, A.; Hu, J.; Lu, J. *J. Zhejiang Univ., Sci.* **2007**, *5*, 830–834.
- (17) Jiang, H.; Kelch, S.; Lendlein, A. *Adv. Mater.* **2006**, *18*, 1471–1475.
- (18) Cho, J. M.; Kim, J. M.; Jung, Y. C.; Goo, N. S. *Macromol. Rapid Commun.* **2005**, *26*, 412–416.
- (19) Mohr, R.; Kratz, K.; Weigel, T.; Lucka-Gabor, M.; Moneke, M.; Lendlein, A. *Proc. Natl. Acad. Sci. U.S.A.* **2006**, *103*, 3540–3545.
- (20) Mornet, S.; Vekris, A.; Bonnet, J. *Mater. Lett.* **2000**, *42*, 183–188.
- (21) Yu, X.; Zhou, S.; Zheng, X.; Guo, T.; Xiao, Y.; Song, B. *Nanotechnology* **2009**, *20*, 1–9.
- (22) Zhou, S.; Deng, X.; Yang, H. *Biomaterials* **2003**, *24*, 3563–3570.
- (23) Sun, J.; Zhou, S. *J. Biomed. Mater. Res., Part A* **2007**, *80*, 333–341.
- (24) Li, F.; Larock, R. C. *J. Appl. Polym. Sci.* **2002**, *84*, 1533–1543.
- (25) Ohki, T.; Ni, Q.; Ohsako, N.; Iwamoto, M. *Composites, Part A* **2004**, *35*, 1065–1073.
- (26) Lepoittevin, B.; Devalckenaere, M. *Polymer* **2002**, *43*, 4017–4023.
- (27) Ahmad, F. N.; Jaafar, M.; Palaniandy, S. *Compos. Sci. Technol.* **2008**, *68*, 346–353.
- (28) Masao, S.; Yasutoshi, T.; Keizo, M. *Mater. Sci.* **1983**, *18*, 1758–1764.
- (29) Scaffaro, R.; Pedretti, U.; Lamantia, F. P. *Eur. Polym. J.* **1996**, *32*, 869–875.
- (30) Zisman, W. A. *Ind. Eng. Chem.* **1963**, *55*, 19–38.
- (31) Eldsäter, C.; Erlandsson, B.; Renstad, R.; Albertsson, A. C.; Karlsson, S. *Polymer* **2000**, *4*, 1297–1304.
- (32) Zheng, X.; Zhou, S.; Yu, X.; Li, X.; Feng, B.; Qu, S.; Weng, J. *J. Biomed. Mater. Res., Part B* **2008**, *86B*, 170–180.
- (33) Elzubair, A.; Elias, C. N.; Suarez, J. C. M.; Lopes, H. P.; Vieira, M. V. B. *J. Dent.* **2006**, *34*, 784–789.
- (34) Göpferich, A. Degradation of biodegradable polymers. Biodegradable polymers—from monomer to the clinic. The 6th World Biomaterials Congress, Hawaii, USA, May 15–20, 2000.

JP9022986